Journal of Histochemistry & Cytochemistry 2021, Vol. 69(6) 415–428

DOI: 10.1369/00221554211022703
journals.sagepub.com/home/jhc
SAGE

Autocrine Hyaluronan Influences Sprouting and Lumen Formation During HUVEC Tubulogenesis In Vitro

Robert B. Vernon, Michel D. Gooden, Christina K. Chan, Gail Workman, Masanari Obika†, and Thomas N. Wight*

Center for Fundamental Immunology, Matrix Biology Program, Benaroya Research Institute at Virginia Mason, Seattle, Washington (RBV, MDG, CKC, GW, MO, TNW)

Summary

Although many studies have focused on a role for hyaluronan (HA) of interstitial extracellular matrix (presumably produced by non-vascular "stromal" cells) in regulating vascular growth, we herein examine the influence of "autocrine HA" produced by vascular endothelial cells themselves on tubulogenesis, using human umbilical vein endothelial cells (HUVECs) in angiogenic and vasculogenic three-dimensional collagen gel cultures. Relative to unstimulated controls, tubulogenic HUVECs upregulated HAS2 mRNA and increased the synthesis of cell-associated HA (but not HA secreted into media). Confocal microscopy/immunofluorescence on cultures fixed with neutral-buffered 10% formalin (NBF) revealed cytoplasmic HAS2 in HUVEC cords and tubes. Cultures fixed with NBF (with cetylpyridinium chloride added to retain HA), stained for HA using "affinity fluorescence" (biotinylated HA-binding protein with streptavidin-fluor), and viewed by confocal microscopy showed HA throughout tube lumens, but little/no HA on the abluminal sides of the tubes or in the surrounding collagen gel. Lumen formation in angiogenic and vasculogenic cultures was strongly suppressed by metabolic inhibitors of HA synthesis (mannose and 4-methylumbelliferone). Hyaluronidase strongly inhibited lumen formation in angiogenic cultures, but not in vasculogenic cultures (where developing lumens are not open to culture medium). Collectively, our results point to a role for autocrine, luminal HA in microvascular sprouting and lumen development. (J Histochem Cytochem 69: 415–428, 2021)

Keywords

angiogenesis, collagen gel, hyaluronan synthase, hyaluronidase, 4-methylumbelliferone, vasculogenesis

Introduction

The glycosaminoglycan hyaluronan (HA) is a long, non-branching polymer of repeating disaccharides of N-acetyl glucosamine and glucuronic acid (GlcUA). HA is an important structural component of the extracellular matrix (ECM) of many tissues, where it regulates tissue hydration and osmotic balance,[1] contributes to tissue viscoelasticity and lubrication, and serves as a scaffold for support of HA-associated proteins and proteoglycans (hyaladherins).[2] In addition to a structural role, HA binds to cell surface receptors to regulate a variety of cell behaviors (e.g., proliferation, motility, adhesion) involved in blood vessel growth, wound repair, tumor metastasis, inflammation, and other processes.[3–6] HA is synthesized by hyaluronan synthases (HASes), which, in mammals, exist in three isoforms (HAS1, HAS2, HAS3).[7] In healthy tissues, HA is present as a high-molecular-weight (> ~1000 kDa) (HMW-HA) polymer, but in inflammation or infection, HA is degraded by mechanical forces, oxidation, and hyaluronidases[8] into shorter chains of relatively low-molecular-weight (<500–700 kDa) (LMW-HA) polymer and HA oligosaccharides (o-HA). A number of studies have contributed to the concept that HMW-HA suppresses inflammation, whereas LMW-HA and o-HA are proinflammatory[4,5,9,10]; however, other studies have called the validity of this idea into question.[11–14]

Received for publication February 17, 2021; accepted May 18, 2021.

†In memoriam.
*Member of The Histochemical Society at the time of publication.

Corresponding Author:
Robert B. Vernon, Center for Fundamental Immunology, Benaroya Research Institute at Virginia Mason, 1201 Ninth Avenue, Seattle, WA 98101-2795, USA.
E-mail: rvernon@benaroyaresearch.org

Journal of Histochemistry & Cytochemistry

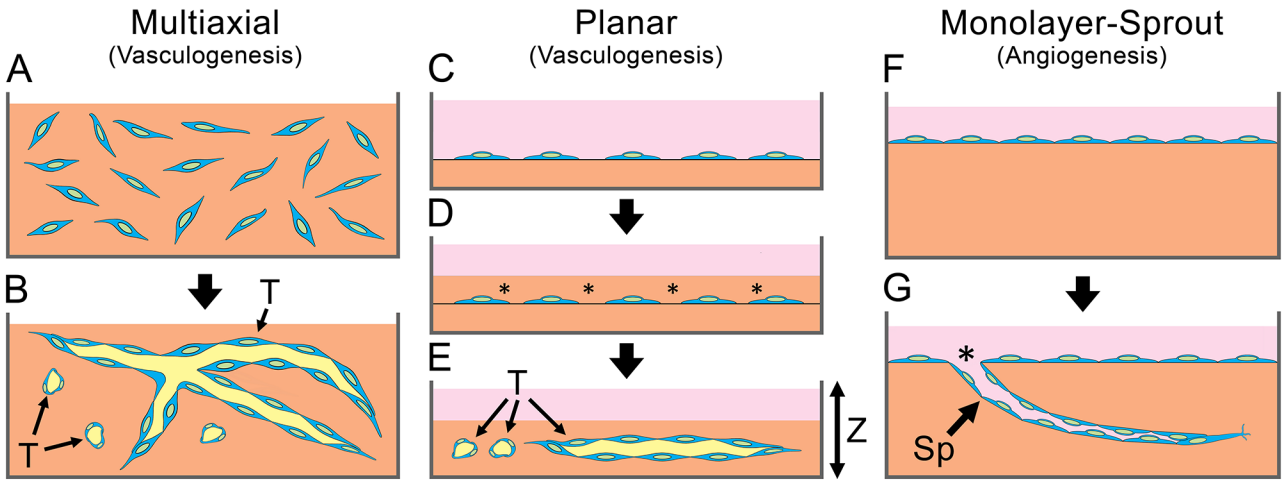

Figure 1. In vitro models of HUVEC tubulogenesis. (A, B) Multiaxial vasculogenesis. (A) Cells (blue) are dispersed in a three-dimensional collagen gel (orange). (B) T-medium induces formation of tubes (T) with patent lumens (yellow) oriented randomly in all three axes. (C–E) Planar vasculogenesis. (C) Subconfluent monolayer of cells is grown on top of a collagen gel (orange) covered with medium (pink). (D) A second layer of collagen (asterisks) is gelled on top of the cells. (E) T-medium induces formation of tubes (T) in a single plane of depth (*Z*-axis). (F, G) Monolayer-sprout angiogenesis. (F) Confluent HUVEC monolayer on top of a collagen gel (orange). (G) T-medium induces the monolayer to produce sprouts (Sp) that enter the collagen. Sprout lumens are open to the culture medium (pink) at the "sprout throat" (asterisk). Abbreviations: HUVEC, human umbilical vein endothelial cell; T-medium, tubulogenesis medium.

Many studies of the influence of HA on vascular growth (vasculogenesis/angiogenesis) have focused on exposure of intact vasculature in vivo or of endothelial cells (ECs) in vitro to purified forms of HMW-HA or its degradation products. Such studies, which report anti-angiogenic[15] and proangiogenic[16–19] effects by HMW-HA and o-HA, respectively, have sought to explain how different forms of HA present in interstitial ECM (presumably produced by non-vascular "stromal" cells) affect blood vessel growth. Beyond such a role for interstitial HA, less attention has been directed to investigating the potential for HA produced by ECs themselves ("autocrine HA") to influence vascular growth and morphogenesis. In this context, this study examines the HA produced by human umbilical vein ECs (HUVECs) undergoing tubulogenesis in three-dimensional (3D) collagen gel culture systems that model vasculogenesis and angiogenesis. The results of the study point to an unexpected role for EC-derived HA in the processes of lumen formation and vascular sprouting.

Materials and Methods

HUVEC Source and Culture Media

For routine culture, pooled HUVECs (Lonza America, Inc.; Allendale, NJ) were grown in a "base medium" consisting of complete EGM-MV2 medium (Lonza) supplemented with 100 U/ml of penicillin and 100 µg/ml of streptomycin. Medium to induce HUVEC tubulogenesis ("T-medium") consisted of EGM-MV2 base medium with a lower concentration (1%) of fetal bovine serum (FBS), 30 ng/ml of recombinant human basic fibroblast growth factor (bFGF) (PeproTech, Inc.; Rocky Hill, NJ), 30 ng/ml of recombinant human vascular endothelial growth factor $(VEGF)_{165}$ (PeproTech), and 100 ng/ml of phorbol 12-myristate 13-acetate (PMA) (Sigma-Aldrich; St. Louis, MO).[20] HUVECs were used for experiments at passage 6 or less.

Tubulogenesis by HUVECs cultured in contact with 3D collagen gels was induced from dispersed cells (a vasculogenic model—Fig. 1A–E) or from confluent monolayers (an angiogenic model—Fig. 1F and G), as described below.

Tubulogenesis From Dispersed HUVECs

"Multiaxial" HUVEC cultures (Fig. 1A and B) used for confocal imaging were established using a nylon mesh ring support system that facilitates handling, cell staining, and imaging (Fig. 2A–C).[21] A 2.5-mg/ml collagen solution was prepared by combining 1 volume of rat tail type I collagen stock (BD Biosciences; Bedford, MA), 1/9 volume of 10-strength Medium 199 (Sigma-Aldrich), 1% FBS, and base medium (added q.s.). HUVECs were dispersed in the collagen solution at 1×10^6 cells/ml and applied in 150 µl volumes to custom-made rings (Sefar America, Inc.; Monterey Park, CA) made from woven Nitex nylon 250/50 mesh (a simple over/under weave with 250 µm square openings comprising 50% of the total mesh area). Outer and inner diameters of each ring were 12.6 and 7.9 mm, respectively (Fig. 2A).[21] The collagen was then polymerized for 30 min in a 37C/5% CO_2

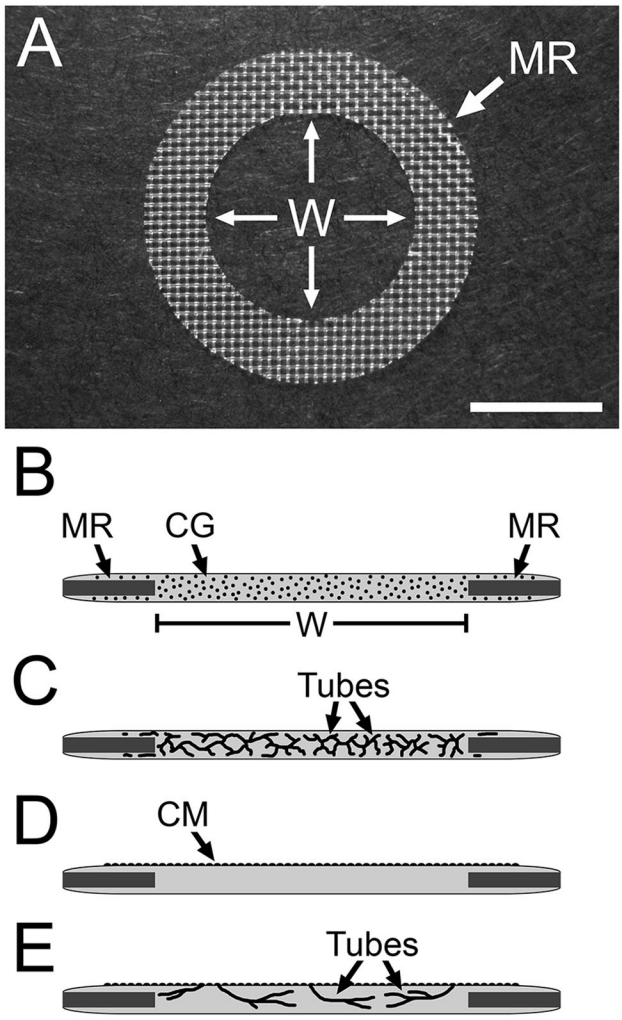

Figure 2. Nylon mesh ring system used to study HUVEC tubulogenesis. (A) Image of a nylon mesh ring (MR) on which the collagen gel is cast. HUVEC tubes that form in the collagen gel are viewed in the central "window" region (W) of the gel. (B–D) Side-view diagrams of the setup for multiaxial (B, C) and monolayer-sprout (D, E) culture modes. (B) HUVECs (black dots) are dispersed in the collagen gel (CG). Nylon mesh ring (MR) and window region (W) of the collagen gel are indicated. (C) The dispersed cells organize into multiaxial HUVEC tubes in response to T-medium. In monolayer-sprout cultures (D), a confluent monolayer (CM) of HUVECs on top of the collagen gel is induced to sprout into the gel (E). Scale bar size: A = 5 mm. Abbreviations: HUVEC, human umbilical vein endothelial cell; T-medium, tubulogenesis medium.

incubator.[21,22] The collagen gel/ring assemblies were cultured in 24-well plates in T-medium for up to 7 days with a change of medium daily.

To facilitate quantification of lumen formation, dispersed HUVECs were induced to form tubes in a single plane (Fig. 1C–E). To accomplish this, 1 ml of a 2-mg/ml collagen solution was dispensed into each well of Lab Tek two-well chambered coverglasses (Product 155380; Nalge Nunc International, Naperville, IL) and polymerized at 37C. Subsequently, 2×10^5 HUVECs in base medium were plated on top of the collagen and cultured for 3 hr to allow the cells to attach. Subsequently, the medium was removed, 1 ml (per well) of collagen was pipetted on top of the subconfluent cells, and the chambers were cultured for 1 hr to polymerize the collagen overlay. The completed gel "sandwiches" were removed from the Lab Tek chambers, transferred to six-well culture plates, and exposed to T-medium (changed daily) to induce tube formation. The reason for the transfer to culture plates was to ensure a better penetration/exchange of culture medium into the gels after each change of medium, in that (1) the gels were able to free-float in the culture medium of the plate wells, thereby permitting the medium to exchange through the bottoms of the gels as well as their tops, and (2) the plate wells allowed the use of a larger volume of medium per gel. In selected experiments, the cultures (treatment groups) were exposed to T-medium only (control) or T-medium supplemented with 300 μM of 4-methylumbelliferone (4-MU) Na salt (≥98% purity; Product M1508), 20 mM of D-(+)-mannose (cell culture tested), 20 mM of D-(+)-glucose (USP), or 200 U/ml of hyaluronidase (type IV-S from bovine testis, embryo tested; Product H4272) (all from Sigma-Aldrich). Media were changed daily. After 6 days of culture, the gels were fixed overnight with neutral-buffered 10% formalin (NBF) and exposed for 4 hr to 2 μg/ml of propidium iodide (PI) in phosphate-buffered saline (PBS) to label nuclear DNA and cytoplasmic RNA.[23] Luminal area per unit of sprout length (μm^2 per μm) of the tubes that formed in the cultures was measured from wide-field fluorescence images of standardized (1 mm^2) area using National Institutes of Health ImageJ public domain software (https://imagej.nih.gov/ij). Data were collected from five gels per treatment group, using five images per gel and >10 measurements per image, for a total n>250 measurements for each treatment group.

Formation of Tubular Sprouts From Confluent HUVEC Monolayers

Tubular angiogenic sprouts from confluent HUVEC monolayers ("monolayer-sprout cultures") (Fig. 1F and G) were prepared using collagen gel/ring assemblies, but without added cells. HUVECs were plated on the upper surface of the gels, cultured in 24-well plates until confluent (Fig. 2D), and then exposed to T-medium (changed daily). Penetration of the collagen gel by multicellular sprouts from the monolayer (Fig. 2E) was monitored by phase-contrast microscopy. In selected experiments, confluent monolayer cultures (treatment groups) were exposed to T-medium only (control) or to T-medium supplemented with 300 μM of 4-MU, 20 mM of D-(+)-mannose, 20 mM of D-(+)-glucose, or 200 U/ml of hyaluronidase (changed daily). After 6 days

of culture, the gels were fixed overnight with NBF, mounted on slides under coverslips, and sprout number (per gel) and average sprout length measured using ImageJ from high-magnification, phase-contrast images stitched into a single composite image of each gel. Experiments were repeated three times with n=3 gels per treatment group per experiment.

Cytochemical Staining

Routine bright-field microscopy was performed on whole-mounted multiaxial tubulogenic cultures with a Leica DM2500 (Leica Microsystems; Wetzlar, Germany) equipped with a SPOT Insight 4 mpx color CCD camera (Diagnostic Instruments; Sterling Heights, MI) on specimens fixed overnight with NBF and stained with 1% crystal violet. For wide-field epifluorescence microscopy, NBF-fixed specimens were stained with 1 µg/ml of 4,6-diamidino-2-phenylindole (DAPI) to label nuclei and 1 U/ml of Alexa Fluor 568–conjugated phalloidin (Molecular Probes/ThermoFisher Scientific; Waltham, MA) to label cytoplasmic f-actin. Fluorescence was imaged using a Leica DMR microscope equipped with a SPOT RT 1.4 mpx color/monochrome CCD camera (Diagnostic Instruments).

For "affinity fluorescence" (AF) confocal imaging of HA in whole-mounted, multiaxial tubulogenic cultures, the specimens were fixed with NBF supplemented with 1% cetylpyridinium chloride (CPC; Sigma-Aldrich). CPC is a cationic, quaternary ammonium compound that precipitates HA (a polyanion), thereby preventing the HA from diffusing out of whole-mounts fixed with NBF. The fixed specimens were stained overnight with 4 µg/ml of biotinylated HA-binding protein (bHABP) and counterstained with 1 U/ml of Alexa Fluor 568 phalloidin. For immunofluorescence (IF) confocal imaging of HAS2, the whole-mounts were stained with 5 µg/ml of a rabbit polyclonal IgG to a cytoplasmic segment (HEKGPGETDESHKEC) of human HAS2 (Product PA5-25593; Invitrogen/ThermoFisher). Bound bHABP and anti-HAS2 antibodies were visualized, respectively, with Alexa Fluor 488 streptavidin and Alexa Fluor 488 or Alexa Fluor 568 polyclonal anti-rabbit IgG (Molecular Probes). Cell nuclei were stained with TO-PRO-3 Iodide (Molecular Probes). AF/IF-labeled specimens were viewed with a TCS-SP5 II scanning confocal microscope (Leica Microsystems).

Western Blot Assays

The protein target for anti-HAS2 antibody binding to HUVECs was characterized by SDS-PAGE/Western blots of cell extracts. HUVECs grown on tissue culture plastic in T-medium were extracted with a solution consisting of 50 mM Tris, 50 mM NaCl, 1% IGEPAL CA-630, 0.25% Na-deoxycholate, 1 mM phenylmethylsulfonyl fluoride (all from Sigma-Aldrich), and a protease inhibitor cocktail for mammalian cells (Product P8340; Sigma-Aldrich). Protein concentration was determined with a Pierce Coomassie Protein Assay Kit (Product 23200; ThermoFisher). Extracts (40 µg total protein/lane) were resolved on polyacrylamide gels (3.5% stacking/8% separating), transferred to nitrocellulose, and probed with 0.5 µg/ml of the HAS2 antibody in conjunction with IRDye 800CW-conjugated goat anti-rabbit IgG (LI-COR Biosciences; Lincoln, NE). Immunoreactive bands on the blots were visualized using a two-channel (red-green) Odyssey CLx flatbed infrared imager (LI-COR).

HAS mRNA Analyses

For analysis of HAS mRNAs, HUVECs were cultured in base medium to confluence on top of 1-mm-thick collagen gels in 24-well plates. Subsequently, the base medium was replaced with 1 ml of T-medium, which was either removed and discarded immediately ("0 hr") or removed after 1, 3, 5, 10, or 24 hr of culture. After removal of the media, the collagen gels with attached cells were placed in individual 2 ml ceramic-bead homogenization tubes (Product D1032-15; Benchmark Scientific, Sayerville, NJ), each filled with 1 ml of TRIzol Reagent (ThermoFisher). Subsequently, the tubes were shaken for 1 min in a BeadBug homogenizer (Benchmark), and the resulting solutions were collected and stored at –80C until analysis.

To assay mRNA levels, the samples were thawed, mixed with 0.2 ml chloroform, incubated at room temperature for 5 min, and spun at 12,000 × g for 10 min at 4C. The aqueous phase was collected, mixed with an equal volume of 70% ethanol, and purified using EconoSpin columns (Epoch Life Science; Missouri City, TX). The samples were washed with RNA Pre-Wash Buffer followed by RNA Wash Buffer (Zymo Research; Irvine, CA). RNA was eluted with water. cDNA was prepared from the isolated RNA with a High-Capacity cDNA Reverse Transcription Kit (ThermoFisher). Real-time PCR was carried out with TaqMan Gene Expression Master Mix (ThermoFisher) on an Applied Biosystems 7900HT Fast Real-Time PCR System. For each sample, assays were run as technical duplicates. cDNA levels were then expressed as estimated copy numbers (CNs) of mRNA relative to 1×10^5 18S rRNA using the master-template approach.[24] TaqMan probes (ThermoFisher) corresponding to human HAS1 (Hs00758053), HAS2 (Hs00193435), HAS3 (Hs00193436), and eukaryotic 18S rRNA (4319413E) were used.

Assay of HA Production by HUVECs

HUVECs were plated on top of 1-mm-thick collagen gels prepared in 12-well tissue culture plates and allowed to grow to confluence for 3 days in base medium. Subsequently, the cultures were exposed for

3 days either to T-medium or to a "control" medium (EGM-MV2 base medium with 1% FBS, 2 ng each of bFGF and VEGF, but no PMA). Media were changed daily, with addition, on day 3, of 30 μCi/ml of [3H]-glucosamine to radiolabel newly synthesized HA. After 24 hr of labeling, media and cellular fractions were collected separately and digested with 16 μg/ml of pronase from *Streptomyces griseus* (Roche Diagnostics; Indianapolis, IN) in 0.5 M Tris, pH 6.5 for 18 hr at 37C. Following digestion, the pronase was inactivated by heating to 100C for 20 min. Radiolabeled macromolecules were then recovered and separated from unincorporated [3H]-glucosamine by precipitation on nitrocellulose as follows: samples (200 μl) were added to an equal volume of 2% CPC/50 mM NaCl and the solution blotted onto nitrocellulose membranes. The membranes were washed 6× in 2% CPC/50 mM NaCl and once in deionized water, then air-dried at room temperature, and assayed in a scintillation counter. Incorporation of [3H]-glucosamine specifically into HA was measured subtractively, that is, by the reduction in radioactive signal of sample aliquots digested with *Streptomyces* hyaluronidase (2 U/ml) (Sigma-Aldrich) for 24 hr at 37C, before slot blotting.[25]

Statistical Analyses

For statistical analyses, *p* values were calculated with Prism (GraphPad Software, Inc.; San Diego, CA) using paired, two-tailed *t*-tests. Each experiment was repeated at least 3×.

Results

HUVECs Upregulate HAS and HA Synthesis in Response to T-Medium

Initial studies examined the time-course of HAS mRNA expression by HUVECs following a tubulogenic stimulus (exposure to T-medium). Quantitative RT-PCR mRNA assays of confluent HUVEC monolayers cultured on top of collagen hydrogels (Fig. 1F) showed an increase in HAS2 mRNA from non-detectable at 0–1 hr to a significant level of expression (avg. CN 360) at 3 hr. HAS2 mRNA expression declined by 5 hr and was non-detectable at the 10- and 24-hr time points (Fig. 3A). A similar expression profile was seen for HAS3 mRNA, but the peak CN was substantially (~10-fold) lower than that of HAS2 mRNA (Fig. 3A). HAS1 mRNA was not detected at any time point. When similar confluent cultures were maintained for 3 days in T-medium or control medium (changed daily) followed by a 24-hr exposure to [3H]-glucosamine and measurement of radioactivity incorporated into HA (Fig. 3B), both control and T-medium cultures had similar quantities of HA in the culture medium. In

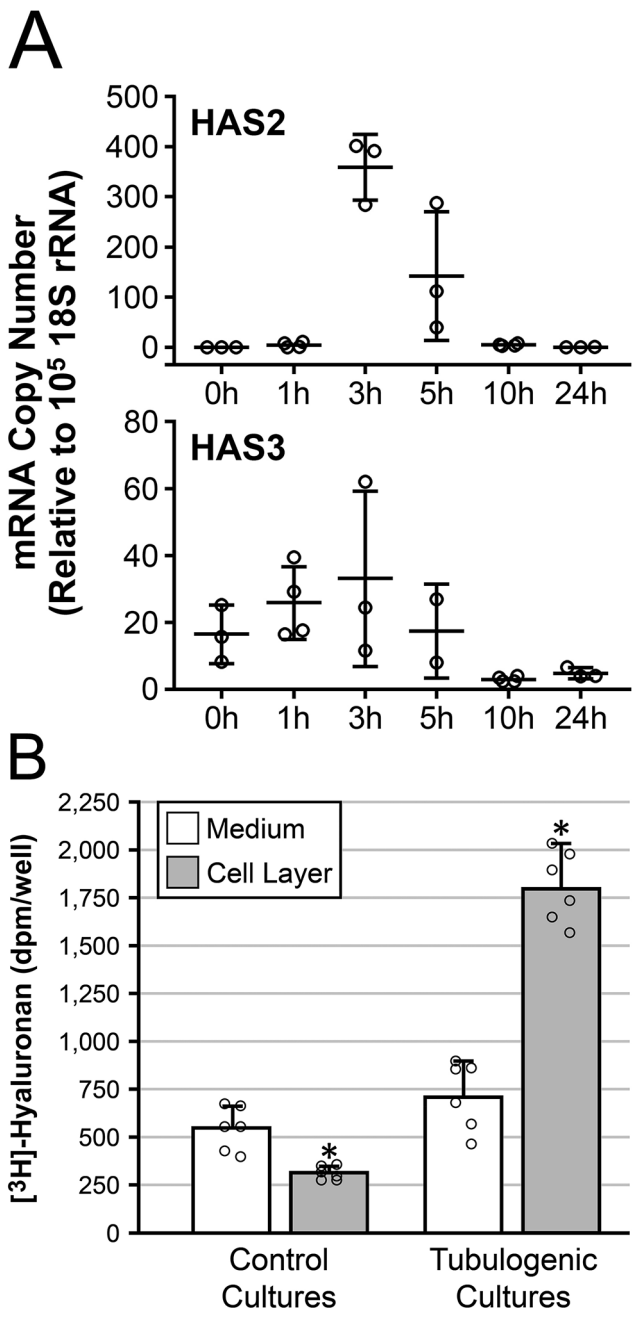

Figure 3. Exposure of HUVECs to T-medium upregulates HAS mRNA and HA. (A) Time-course, following exposure to T-medium, of HAS2 and HAS3 mRNA expression by confluent HUVEC monolayers grown on top of collagen gels. HAS2 (top) and HAS3 (bottom) mRNA both peak at 3 hr. Peak copy number of HAS3 mRNA is ~10-fold lower than that of HAS2. *n*=3 or 4 samples per time point. (B) Cultures similar to those of "A" were exposed for 3 days to control medium (control cultures) or T-medium (tubulogenic cultures) followed by metabolic radiolabeling of HA for 24 hr. Levels of HA secreted into the culture medium (white bars) are similar in both control and tubulogenic cultures. In contrast, the level of HA incorporated into the cell layer (gray bars) is significantly higher in the tubulogenic cultures compared with the control cultures. In this bar graph, individual sample values for the four groups are shown as scatter plots (open circles, *n*=6 per group) superimposed over the bars. Abbreviations: HUVEC, human umbilical vein endothelial cell; HAS, hyaluronan synthase; HA, hyaluronan; T-medium, tubulogenesis medium. *$p<0.001$.

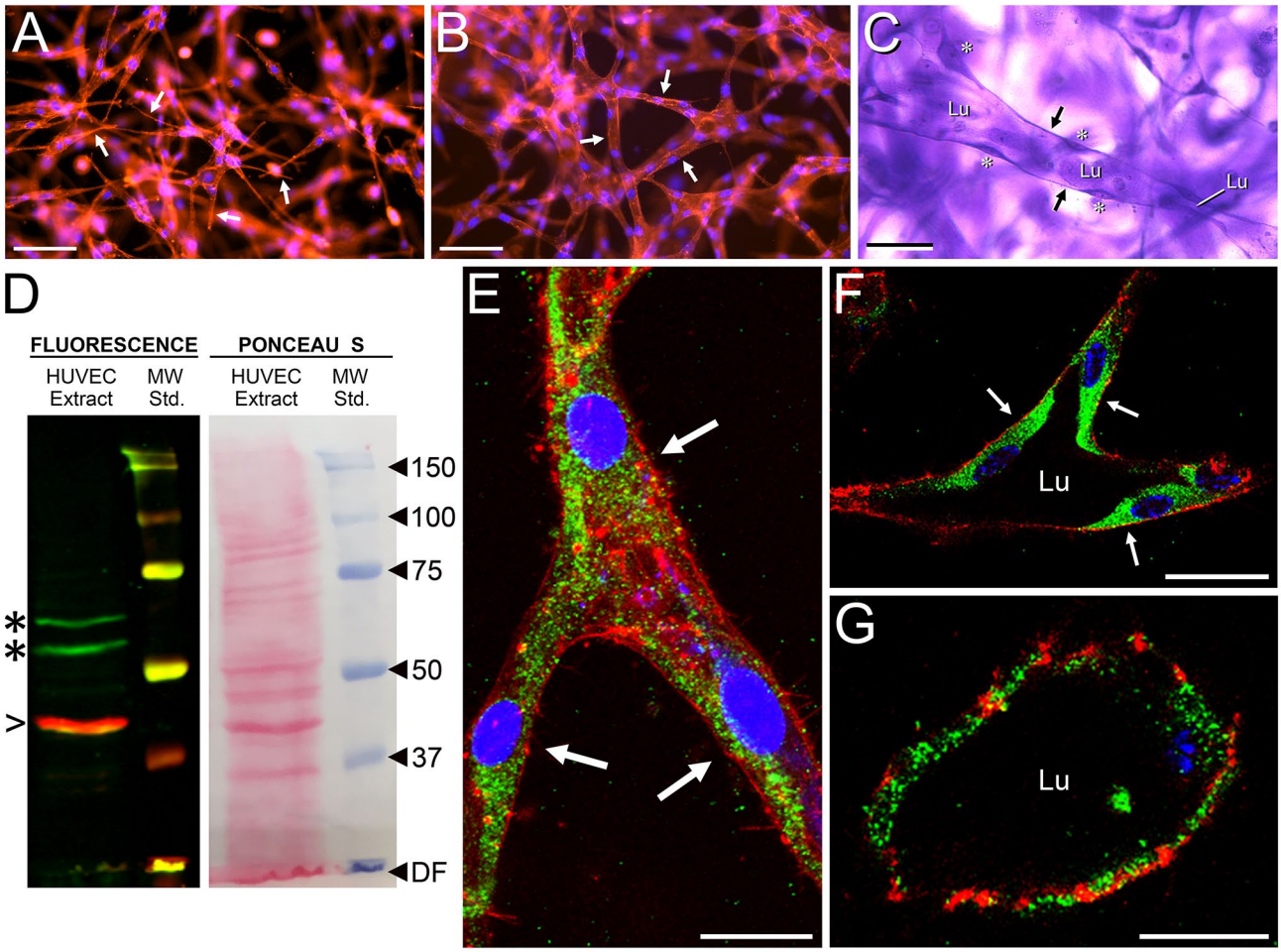

Figure 4. Expression of HAS2 in HUVEC cords and tubes. (A–C) Stages of tube formation in whole-mount, multiaxial vasculogenic cultures, as shown by epifluorescence microscopy in (A) and (B) (red, phalloidin stain for f-actin; blue, DAPI nuclear stain) and bright-field microscopy in (C) (crystal violet stain). At 24 hr (A), cells acquire spindle shapes with long, narrow pseudopodia (e.g., arrows). By 48 hr (B), the cells form a network of multicellular cords (arrows indicate three cords). Appearance of fully developed tubes (one is indicated in C), each with a patent lumen (Lu) and thin walls (arrows), occurs at 3–7 days. Areas of cytoplasm containing nuclei (asterisks) bulge into the lumen. In a Western blot of tubulogenic HUVEC extract (D), anti-HAS2 antibody (green stain) recognizes 53 and 64 kDa bands (asterisks). β-actin (red stain, arrowhead) marks 42 kDa. Ponceau S stain reveals many non-immunoreactive protein bands. (E–G) Whole-mounts of HUVEC cords and tubes in three-dimensional collagen gels evaluated by IF/confocal microscopy for HAS2 (green stain). (E) Cord of a 48-hr culture showing three cells (arrows) at a branch point. (F, G) Cross-sections of large-diameter (F) and small-diameter (G) tubes with patent lumens in a 4-day culture. In (F), arrows indicate the cells comprising the tube wall. In (E)–(G), f-actin is stained with phalloidin (red) and nuclei are stained with TO-PRO-3 (blue). Scale bar sizes: A, B = 100 μm; C = 50 μm; E, F = 10 μm; G = 5 μm. Abbreviations: HUVEC, human umbilical vein endothelial cell; DAPI, 4, 6-diamidino-2-phenylindole; IF, immunofluorescence; DF, dye front; MW, molecular weight.

contrast, the quantity of HA deposited in the cell layer was markedly (> 5.7-fold) higher in the T-medium cultures vs the controls. Of note, most (~72%) of the HA in the T-medium cultures was found in the cell layer (i.e., was cell-associated) rather than in the culture medium (i.e., freely soluble).

Association of HAS2 and HA With Vasculogenic HUVEC Tubes

HUVECs dispersed within a 3D native type I collagen gel and exposed to tubulogenic medium organize into a network of thin-walled, multicellular tubes with relatively wide, fluid-filled lumens that closely resemble native capillaries.[22,26] In this model, tube formation is thought to represent aspects of vasculogenesis and begins when the individual cells acquire spindle shapes within 24 hr (Fig. 4A), organize into a network of multicellular cords within 48 hr (Fig. 4B), and become fully developed tubes with patent lumens and thin walls after 3–7 days (Fig. 4C). Using this model, we subjected whole-mount cultures to AF/IF and confocal microscopy to localize HAS2 and HA within HUVEC tubes. Multiaxial cultures (Figs. 1A

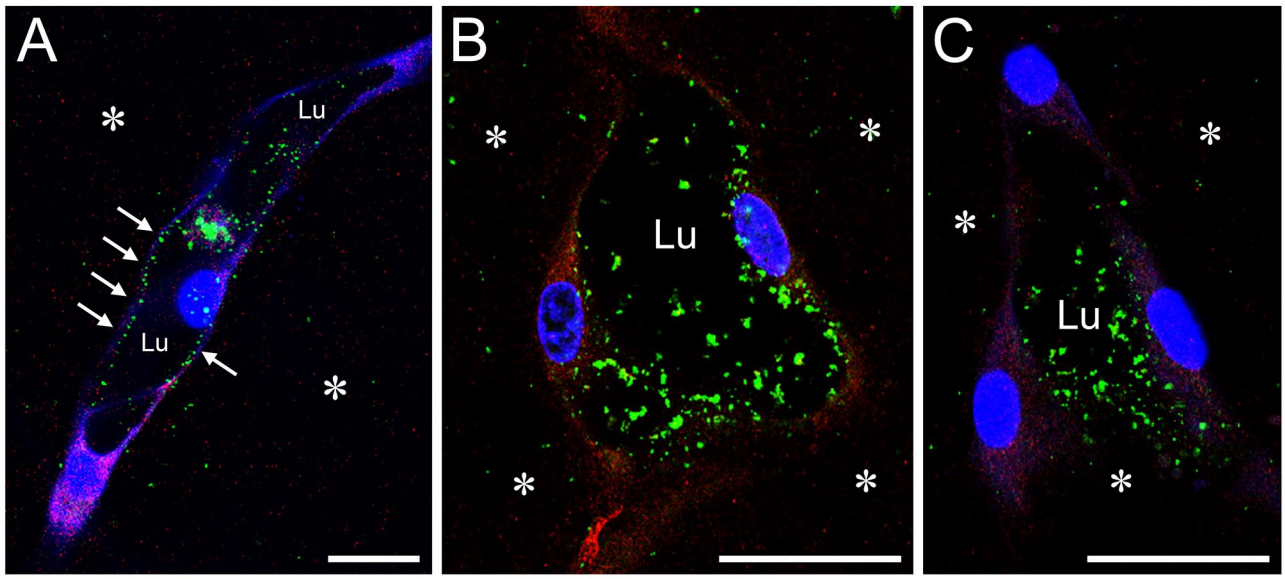

Figure 5. HA is localized to the lumens of HUVEC tubes. HUVEC tubes in whole-mount, multiaxial vasculogenic cultures are viewed by confocal microscopy after AF/IF staining for HA and HAS2. Tubes are imaged in longitudinal (A) and cross-sectional (B, C) planes. Specimens were fixed with NBF with 1% CPC added to precipitate the HA. In (A)–(C), precipitated HA (green) appears as punctate masses in the tube lumens (Lu), in some cases attached to the luminal wall (e.g., A, arrows). HA is largely absent from abluminal EC surfaces. In the supportive collagen gel (asterisks), HA is very scant. The CPC treatment has reduced the IF signal for HAS2, resulting in a relatively weak red staining of cytoplasm, but the staining reveals that HA is generally absent from the cytoplasm. In all images, cell nuclei are stained with TO-PRO-3 (blue). Scale bar sizes: A–C = 10 µm. Abbreviations: HA, hyaluronan; HUVEC, human umbilical vein endothelial cell; AF, affinity fluorescence; IF, immunofluorescence; NBF, neutral-buffered 10% formalin; CPC, cetylpyridinium chloride; EC, endothelial cell.

and B, and 2B and C) were used, as both cross-sectional and longitudinal section views are easily found in the same specimen. Before IF for HAS2, we evaluated HAS2 antibody reactivity to HUVECs by Western blot (Fig. 4D). The antibody we selected recognized two bands of 53 and 64 kDa, which corresponded to previously published HUVEC Western blots labeled with a different anti-HAS2 antibody.[27] In the present study, HAS2 was strongly expressed in multicellular cords, appearing as aggregates of puncta (Fig. 4E). A similarly robust, punctate expression in cytoplasm was observed in HUVECs that had formed tubes with patent lumens (Fig. 4F and G). AF staining for HA showed HA to be concentrated in the lumens of the tubes. This luminal HA was revealed by incorporating CPC into the fixative, which promoted retention of the HA in the specimens during processing for AF/IF (see section "Cytochemical Staining"). The stained HA appeared as brightly fluorescent, punctate precipitates dispersed throughout the tube lumens and also attached to the luminal wall (Fig. 5), with essentially no HA present on the EC abluminal surfaces and very scant HA in the supportive collagen gel. In the absence of CPC treatment of the specimens, luminal HA staining appeared as a barely detectable uniform fluorescence (data not shown).

Effect of Inhibitors of HA Accumulation on Lumen Formation by Vasculogenic HUVECs

Given the accumulation of HA in the lumens of vasculogenic HUVEC tubes, we evaluated the effects of hyaluronidase and of inhibitors of HA synthesis (mannose and 4-MU) on the development of lumens in these cultures. Mannose inhibits HA production by specifically reducing cellular pools of HA precursor UDP-*N*-acetylhexosamines,[28] whereas 4-MU reduces pools of the other building block of HA synthesis, UDP-GlcUA, by covalently attaching (via UDP-GlcUA transferase catalysis) to UDP-GlcUA and reducing its available concentration.[28,29] In our studies, we supplemented T-medium with concentrations of 4-MU (0.3 mM)[30–33] and mannose (20 mM)[28,34] known to inhibit HA synthesis in cultured cells. To control for potential osmotic effects of mannose and its function as an energy supply,[28] HUVECs were also cultured in 20 mM (high)-glucose T-medium (the control T-medium contained 5.77 mM glucose).

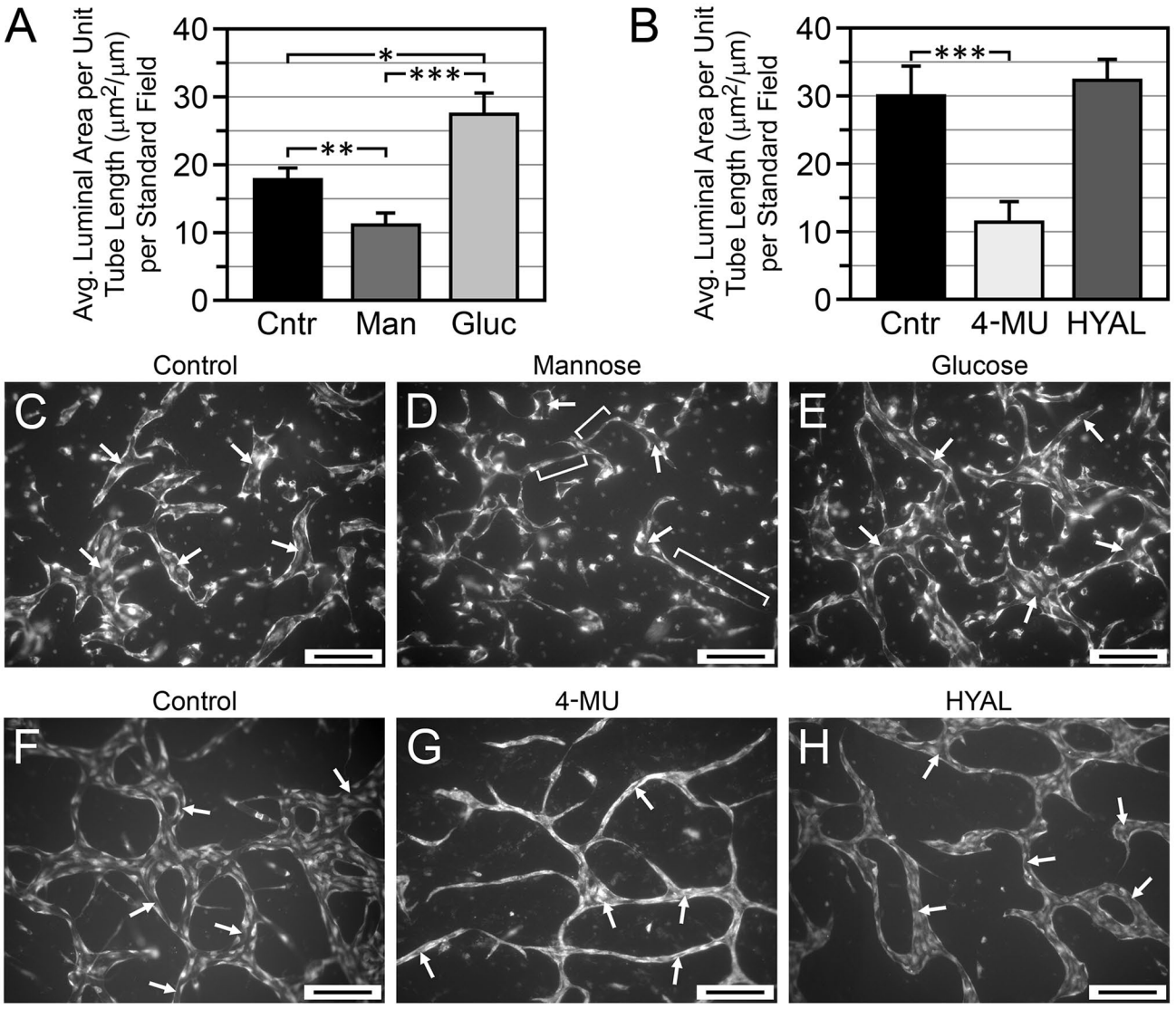

Figure 6. Effects of inhibitors of HA accumulation on lumen formation in vasculogenic HUVEC cultures. (A, B) Analysis of lumen size (caliber) in cultures grown 6 days in T-medium with no additives (control = Cntr) or supplemented with 20 mM mannose (Man), high (20 mM) glucose (Gluc), 0.3 mM 4-MU, or 200 U/ml hyaluronidase (HYAL). In (A), *p=0.02 Cntr vs Gluc; **p<0.02 Cntr vs Man; ***p<0.002 Gluc vs Man. In B, ***p<0.001 Cntr vs 4-MU. In (A) and (B), n>250 per treatment group. (C–E) Representative images of control (C), mannose-treated (D), and high-glucose-treated (E) cultures. (F–H) Representative images of control (F), 4-MU-treated (G), and HYAL-treated (H) cultures. Arrows in (C)–(H) indicate examples of tube lumens. Brackets in (D) indicate examples of narrow cords with very limited luminal development. Compared with controls, lumen caliber was significantly decreased by mannose and 4-MU, significantly increased by high glucose, and not significantly affected by HYAL. Images (C)–(H) are of PI-stained whole-mounts viewed by wide-field epifluorescence. Scale bar sizes: C–H = 200 μm. Abbreviations: HA, hyaluronan; HUVEC, human umbilical vein endothelial cell; 4-MU, 4-methylumbelliferone; PI, propidium iodide; T-medium, tubulogenesis medium.

Three-dimensional vasculogenic HUVEC cultures forming tubes in a single plane (Fig. 1C–E) were used to facilitate measurement of lumen dimensions from photomicrographs. Measurements were rendered as average luminal area per unit tube length (μm²/μm), which characterizes lumen development in terms of average width (caliber), independent of the tube length. Lumen caliber in 6-day cultures was significantly decreased by mannose, relative to both the high-glucose and control T-media (Fig. 6A and C–E). Also of note, HUVECs grown in high-glucose T-medium developed lumens with significantly greater caliber than HUVECs grown in control T-medium (Fig. 6A, C, and E). Lumen formation was strongly inhibited by 4-MU (Fig. 6B)—these cultures organized into cord-like structures with very narrow lumens (Fig. 6G), relative

to controls (Fig. 6F). Interestingly, compared with controls, lumen caliber was not significantly affected by treatment with a high concentration (200 U/ml) of hyaluronidase (Fig. 6B and H).

Effect of Inhibitors of HA Accumulation on HUVEC Sprouting

After the studies of vasculogenic HUVEC cultures, we evaluated the influence of inhibitors of HA accumulation on the formation of sprouts by HUVECs cultured under conditions that model angiogenesis. In these "monolayer-sprout" cultures (Fig. 1F and G), the sprouts grow from a confluent EC monolayer into an underlying 3D collagen gel.[35,36] The sprouts maintain contact with the EC monolayer, and each sprout lumen is open to the overlying culture medium via a sprout "throat" (Fig. 1G, asterisk). We used a collagen gel of limited thickness (Fig. 2D and E), which causes the sprouts to lie parallel to the overlying monolayer, allowing sprout number, sprout length, and lumen development to be readily assessed by phase-contrast microscopy.

Monolayer-sprout cultures grown 6 days in T-medium supplemented with 20 mM mannose, 0.3 mM 4-MU, or 200 U/ml hyaluronidase formed significantly fewer sprouts than cultures grown in control T-medium without these additives, but, interestingly, sprout numbers were significantly increased in the presence of high glucose (Fig. 7A and B). Of the sprouts that formed in all of these cultures, sprout length was not affected by mannose, 4-MU, or high glucose relative to controls (Fig. 7C), but was significantly reduced by hyaluronidase (Fig. 7D). In similarity to the vasculogenic cultures, the tubes formed by the monolayer-sprout cultures contained HA in their lumens (Fig. 8A). Sprouts in control cultures had well-developed lumens that extended from the pore throat to the tips of the sprout (Fig. 8B). Compared with the controls, however, sprouts that formed in the presence of 0.3 mM 4-MU or 20 mM mannose had poorly developed, discontinuous lumens, which appeared as narrow channels or single/clustered vacuoles (Fig. 8C and D). Sprouts that formed in the presence of high glucose (Fig. 8E) had well-developed lumens that were at least as large as those of the controls. Interestingly, in contrast to the vasculogenic cultures, hyaluronidase strongly inhibited lumen formation in monolayer-sprout cultures (Fig. 8F).

Discussion

This study shows that exposure of HUVECs to a tubulogenic environment in vitro results in an increased production of HA, which is accompanied by a transient upregulation of HAS2 mRNA. Most of the newly produced HA remains associated with the cells rather than being released freely into the surrounding medium. In the context of this cell-associated HA, AF/confocal microscopy of whole-mount HUVEC cultures, treated with CPC to preserve HA, revealed abundant HA in the lumens of HUVEC tubes. Of particular significance, a substantial portion of this HA occupied the central lumen rather than being restricted only to the luminal surface of the ECs in a classical vascular glycocalyx.[37,38]

In contrast to the presence of HA in HUVEC tube lumens, we did not detect HA on the exterior of HUVEC tubes, which may reflect the reported absence of an abluminal polysaccharide layer near the growing tips of neovessels in vivo.[37] The absence of abluminal HA on our HUVEC tubes does not, by itself, indicate a complete absence of an exterior cell coat, as we have previously shown that biglycan is present on the exterior surfaces of these tubes.[20] It is noteworthy that HA production differs significantly among different cell types; for example, cultured human bronchial epithelial cells (BECs) produce 20-fold less HA than cultured human lung fibroblasts.[39] Like BECs, we observe that cultured HUVECs produce relatively small amounts of HA—particularly secreted, freely soluble HA that could contribute to interstitial ECM (unpublished observations). Such a wide, cell type–specific variation in levels of HA synthesis underscores the concept that HA is a multifunctional molecule with roles extending beyond bulk structural support to include more subtle, targeted effects on cell behavior.

The formation of vascular sprouts with patent lumens is a complex process involving multiple molecular and biomechanical mechanisms, which include cell surface receptor–mediated signaling, cytoskeletal involvement, cell rearrangement, integrin engagement of surrounding ECM, and ECM proteolysis.[36,40–43] In direct association with these mechanisms is the development of nascent luminal spaces by intracellular vacuolization, which has been shown to occur both in vivo and in vitro.[36,40,43] In vitro, vacuolization within isolated ECs occurs in vasculogenic models and in angiogenesis-like scenarios when ECs sprout from confluent monolayers into underlying ECM.[36,40] These vacuoles can be labeled with membrane-impermeant dyes, indicating that pinocytosis plays a role in their formation.[26] Once formed, the intracellular vacuoles expand, exocytose, and contribute to the developing luminal surface. Participation of neighboring cells in this process is thought to be an important factor in the formation of a multicellular tube.[40]

At this point in the discussion, it is important to note that in vitro models of vascular tubulogenesis, which include the ones used in this study, are artificial

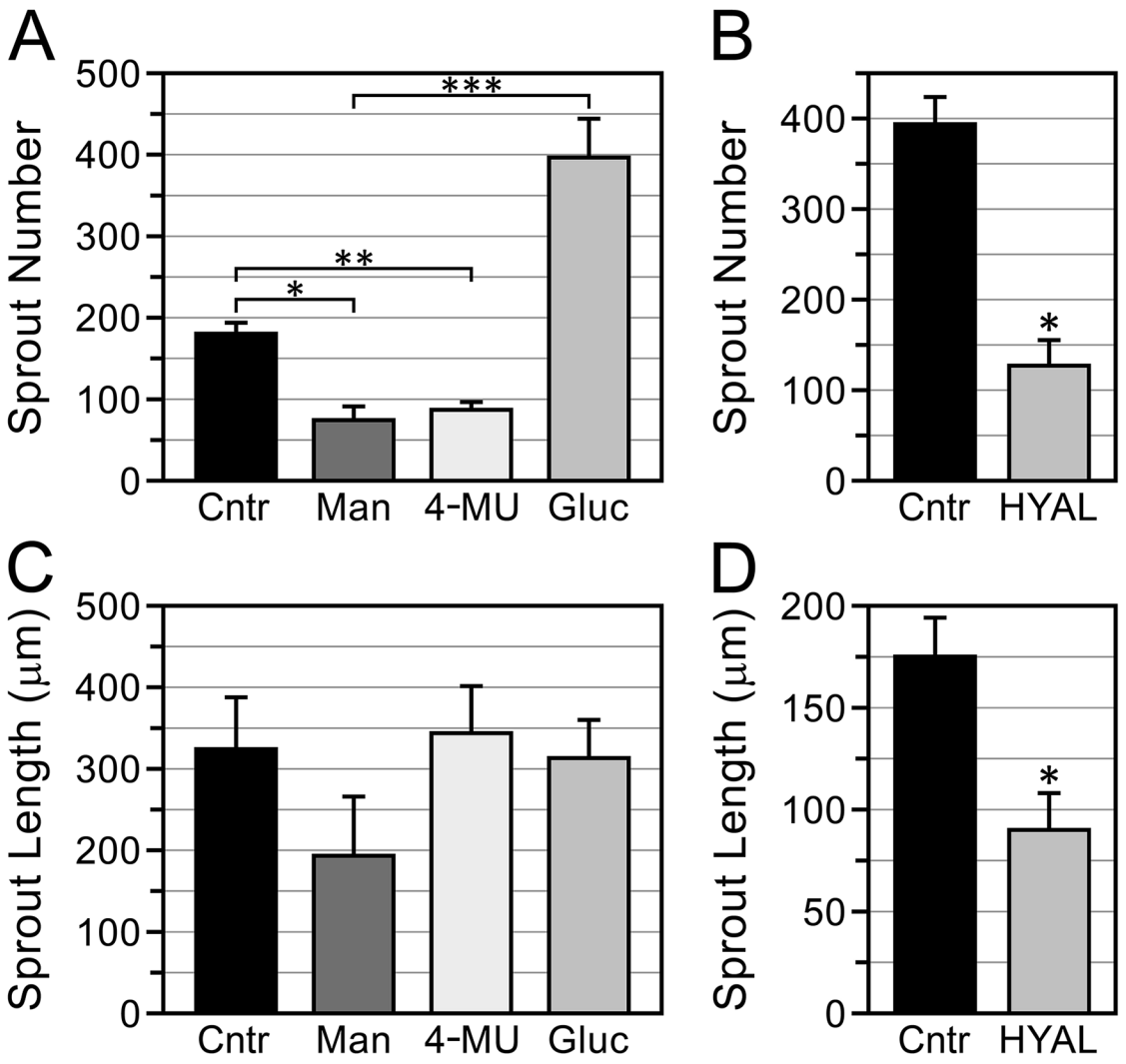

Figure 7. Inhibitors of HA accumulation influence HUVEC sprouting. (A, B) Assays of sprouts produced by monolayer-sprout cultures grown 6 days in T-medium with no additives (control—Cntr) or supplemented with 20 mM mannose (Man), 0.3 mM 4-MU, high (20 mM) glucose (Gluc), or 200 U/ml of hyaluronidase (HYAL). (A, B) Compared with controls, sprout numbers were significantly reduced by mannose, 4-MU, and hyaluronidase, but significantly increased by high glucose. (C, D) Compared with controls, sprout length was not affected by mannose, 4-MU, or high glucose (C), but was significantly decreased by hyaluronidase (D). In (A)–(D), n=3 cultures for each treatment group. Abbreviations: HA, hyaluronan; HUVEC, human umbilical vein endothelial cell; 4-MU, 4-methylumbelliferone; T-medium, tubulogenesis medium. (A) *p<0.05. **p<0.04. ***p<0.03; (B) *p<0.001; (D) *p<0.01.

systems that do not reproduce all of the factors that exist in angiogenic or vasculogenic environments in vivo. For example, in vitro models generally do not reproduce the intraluminal pressure and flow elements (i.e., flowing blood) present in "parent" vessels from which neovessels form by angiogenesis. In addition, the 3D supportive gels (typically made from collagen, fibrin, or basement membrane matrix) used in tubulogenesis models do not fully simulate native interstitial ECM in terms of its molecular complexity or biomechanical properties (e.g., the presence of interstitial fluid pressure or forces of traction, tension, or compression acting on ECM under typical mechanical loads). Therefore, any observations or conclusions regarding neovascular morphogenesis that are made using in vitro models should, eventually, be evaluated in an in vivo setting.

The results of this study point to a role for autocrine, EC-derived HA in vascular lumen formation. We observed that the development of lumens in vasculogenic tubes formed by dispersed HUVECs and in tubular angiogenic sprouts formed by confluent HUVEC monolayers was markedly suppressed in the presence of metabolic inhibitors of HA production, such as mannose or 4-MU. Underscoring the importance of luminal HA in lumen development are the

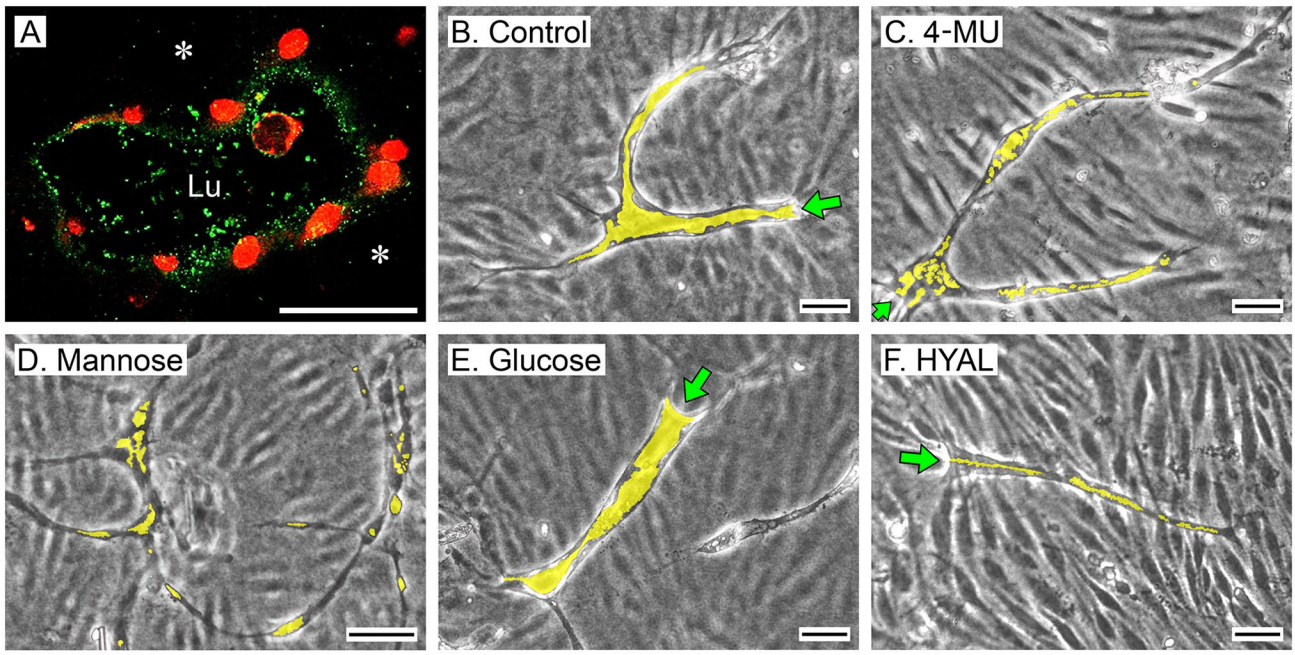

Figure 8. Inhibitors of HA accumulation suppress lumen development in HUVEC sprouts. (A) Confocal image (cross-section) of a sprout in a 6-day monolayer-sprout culture (control) fixed with NBF/1% CPC and then stained by AF (green) to visualize HA in the tube lumen (Lu). HA is scant in the supportive collagen gel (asterisks). Sprout nuclei are stained with PI (red). (B–F) Phase-contrast images of sprouts in 6-day tubulogenic monolayer cultures receiving T-medium with no additives (B, control) or supplemented with 0.3 mM 4-MU (C), 20 mM mannose (D), high (20 mM) glucose (E), or 200 U/ml hyaluronidase (HYAL). (F). Sprouts are seen against out-of-focus backgrounds of the confluent cell monolayers located above them. Compared with controls, luminal areas of sprouts (yellow shading) are substantially reduced and discontinuous in the 4-MU, mannose, and hyaluronidase-treated cultures. Lumens in the high-glucose-treated cultures are at least as large as controls. In the phase-contrast images, sprout throats are indicated by green arrows. Scale bar sizes: A = 10 μm; B, C, E, F = 50 μm; D = 100 μm. Abbreviations: HA, hyaluronan; HUVEC, human umbilical vein endothelial cell; NBF, neutral-buffered 10% formalin; CPC, cetylpyridinium chloride; AF, affinity fluorescence; PI, propidium iodide; 4-MU, 4-methylumbelliferone; T-medium, tubulogenesis medium.

effects of the HA-degrading enzyme hyaluronidase—we found that hyaluronidase robustly suppressed lumen formation in HUVEC monolayer-sprout cultures, but did not inhibit lumen formation in tubes generated by dispersed HUVECs. This discrepancy could be explained in terms of access of the hyaluronidase in the culture medium to the luminal compartment, that is, in monolayer-sprout cultures the lumens of the developing tubes are always open to the overlying culture medium via their throats (Fig. 1G), whereas tubulogenesis by dispersed HUVECs involves the formation of solid cords of cells before lumen development (Fig. 4B) which may act as a barrier separating the hyaluronidase in the culture medium from the zones within the cord where vacuoles form and coalesce.

At present, the means by which endogenous HA could contribute to lumen development is not clear. Purified o-HA is reported to stimulate EC proliferation, migration, secretion of angiogenic factors, and overall vascular growth via receptor-mediated (e.g., CD44/RHAMM) signaling,[38,44] although the direct involvement of o-HA in lumen development has not been established. Of note, there are concerns that some of the biological effects of LMW-HA/o-HA (e.g., induction of inflammatory responses) may be the consequence of contamination with endotoxin,[14] which has been shown to elicit proangiogenic behaviors in ECs.[45–48]

Of note, we found that in situations where 4-MU, mannose, and hyaluronidase inhibit lumen development, vacuoles or lumens of narrow caliber still form, but do not expand. In this context, the hygroscopic properties of HA make this molecule an ideal agent to contribute to the enlargement of intracellular vacuoles and, following vacuolar exocytosis, promote the overall expansion of the nascent lumen. HA has a substantial capacity to interact with water molecules, occupying a large hydrodynamic volume in solution—a property that allows HA to regulate tissue hydration and osmotic balance in extracellular compartments.[1] HA is well suited as a medium to exert hydraulic pressure extracellularly or for intracellular vacuolar expansion—the osmotic pressure of HA is substantially higher than a soluble protein, such as serum albumin, on a weight to volume basis,[49] permitting HA to generate substantial

osmotic pressures at relatively low concentrations. Moreover, osmotic pressures of HA solutions are non-ideal, that is, with increased concentration of HA, osmotic pressures increase exponentially rather than linearly, as solutions of serum albumin do.[49] Therefore, moderate changes in HA concentration could lead to marked increases in osmotic pressure.[50] Of note, polyionic polysaccharides such as HA alter their conformation with changes in type or concentration of counterions in their vicinity.[49] As cationic strength is lowered, the anionic charges of HA repel one another and the molecule expands to a more extended conformation,[51–53] thereby (it has been proposed) converting changes in counterion concentration to mechanical energy.[49,54] In this context, during EC lumen formation, accumulation of HA might contribute to the expansion of vacuoles by not only increasing vacuolar osmotic pressure, but also by direct expansion of the polyanionic HA molecules as cation concentration decreases upon water influx. Significantly, a previous report[55] indicates a role for saccharide-mediated anionic electrostatic repulsion in initiating vascular lumen formation—accumulation of sialic acid (bound to glycoproteins and/or proteoglycans at EC surfaces) may help start lumen formation by pushing apart apposing cells within solid EC cords. Beyond this event, mechanical work (via electrostatic and/or osmotic forces) performed by accumulation of luminal HA might contribute to further expansion of the nascent lumen.

In addition to contributing to lumen development, endogenous HA appears to be involved in the process of sprout initiation, as we observe that confluent HUVEC monolayers cultured on top of collagen gels produce significantly fewer sprouts in the presence of mannose or 4-MU. Similarly, hyaluronidase inhibits sprouting. Whether or not endogenous HA influences sprout initiation via focal changes in osmotic pressure, electrostatic repulsion, or by other mechanisms (e.g., influences over the invasion of the collagen gel by leading tip cells) remains to be determined.

Observations in vivo that 4-MU treatment suppresses vascularization of tumors and endometriotic lesions[56–58] support the concept of using inhibition of HA synthesis as a therapy to treat neovascularization-dependent disease processes. In these therapeutic scenarios, antiangiogenic effects of 4-MU might involve inhibition of "stromal HA" production by non-vascular cells—in tumor progression, stromal HA is thought to provide a microenvironment that supports recruitment of inflammatory cells that can release angiogenic growth factors.[59] Stromal HA may also be a source of proangiogenic oligosaccharides.[60] However, beyond the involvement of stromal HA, the present study suggests that HA-suppressive therapies might also target ECs directly—inhibiting the accumulation of EC-derived HA in nascent luminal compartments in a manner that suppresses both sprout initiation and sprout morphogenesis.

Acknowledgments

The authors thank John A. Gebe, PhD, for statistical suggestions and Virginia M. Green, PhD, for editorial assistance.

†In Memoriam

This study is dedicated to the memory of our friend and colleague Masanari (Masa) Obika, MD, who, as a Visiting Scientist in the Matrix Biology Program at the Benaroya Research Institute, made many important observations that contributed to this work. Masa's insight, team spirit, cheerfulness, and caring nature will remain in our memory always.

Competing Interests

The author(s) declared no potential conflicts of interest with respect to the research, authorship, and/or publication of this article.

Author Contributions

RBV designed the study and drafted the manuscript; RBV, MDG, CKC, GW, and MO conducted the experiments; RBV and TNW managed the project. All authors have read and approved the manuscript before submission.

Funding

The author(s) disclosed receipt of the following financial support for the research, authorship, and/or publication of this article: This project was supported by a major grant from the Klorfine Foundation (RBV) and by NIH grant R01 EB012558 (RBV/TNW). The funding sources had no involvement in study design; in the collection, analysis, and interpretation of data; in the writing of this article; or in the decision to submit this article for publication.

Literature Cited

1. Tammi MI, Day AJ, Turley EA. Hyaluronan and homeostasis: a balancing act. J Biol Chem. 2002;277:4581–4.
2. Karamanos NK, Piperigkou Z, Theocharis AD, Watanabe H, Franchi M, Baud S, Brezillon S, Gotte M, Passi A, Vigetti D, Ricard-Blum S, Sanderson RD, Neill T, Iozzo RV. Proteoglycan chemical diversity drives multifunctional cell regulation and therapeutics. Chem Rev. 2018;118:9152–232.
3. Toole BP. Hyaluronan: from extracellular glue to pericellular cue. Nat Rev Cancer. 2004;4:528–39.
4. Jiang D, Liang J, Noble PW. Hyaluronan as an immune regulator in human diseases. Physiol Rev. 2011;91:221–64.
5. Tavianatou AG, Caon I, Franchi M, Piperigkou Z, Galesso D, Karamanos NK. Hyaluronan: molecular size-dependent signaling and biological functions in inflammation and cancer. FEBS J. 2019;286:2883–908.

6. Garantziotis S, Savani RC. Hyaluronan biology: a complex balancing act of structure, function, location and context. Matrix Biol. 2019;78–79:1–10.
7. Torronen K, Nikunen K, Karna R, Tammi M, Tammi R, Rilla K. Tissue distribution and subcellular localization of hyaluronan synthase isoenzymes. Histochem Cell Biol. 2014;141:17–31.
8. Stern R, Jedrzejas MJ. Hyaluronidases: their genomics, structures, and mechanisms of action. Chem Rev. 2006; 106:818–39.
9. Ruppert SM, Hawn TR, Arrigoni A, Wight TN, Bollyky PL. Tissue integrity signals communicated by high-molecular weight hyaluronan and the resolution of inflammation. Immunol Res. 2014;58:186–92.
10. Cyphert JM, Trempus CS, Garantziotis S. Size matters: molecular weight specificity of hyaluronan effects in cell biology. Int J Cell Biol. 2015;2015:563818.
11. Krejcova D, Pekarova M, Safrankova B, Kubala L. The effect of different molecular weight hyaluronan on macrophage physiology. Neuro Endocrinol Lett. 2009; 30(Suppl. 1):106–11.
12. Ebid R, Lichtnekert J, Anders HJ. Hyaluronan is not a ligand but a regulator of toll-like receptor signaling in mesangial cells: role of extracellular matrix in innate immunity. ISRN Nephrol. 2014;2014:714081.
13. Huang Z, Zhao C, Chen Y, Cowell JA, Wei G, Kultti A, Huang L, Thompson CB, Rosengren S, Frost GI, Shepard HM. Recombinant human hyaluronidase PH20 does not stimulate an acute inflammatory response and inhibits lipopolysaccharide-induced neutrophil recruitment in the air pouch model of inflammation. J Immunol. 2014;192:5285–95.
14. Dong Y, Arif A, Olsson M, Cali V, Hardman B, Dosanjh M, Lauer M, Midura RJ, Hascall VC, Brown KL, Johnson P. Endotoxin free hyaluronan and hyaluronan fragments do not stimulate TNF-alpha, interleukin-12 or upregulate co-stimulatory molecules in dendritic cells or macrophages. Sci Rep. 2016;6:36928.
15. Feinberg RN, Beebe DC. Hyaluronate in vasculogenesis. Science. 1983;220:1177–9.
16. West DC, Hampson IN, Arnold F, Kumar S. Angiogenesis induced by degradation products of hyaluronic acid. Science. 1985;228:1324–6.
17. Sattar A, Rooney P, Kumar S, Pye D, West DC, Scott I, Ledger P. Application of angiogenic oligosaccharides of hyaluronan increases blood vessel numbers in rat skin. J Invest Dermatol. 1994;103:576–9.
18. Lees VC, Fan TP, West DC. Angiogenesis in a delayed revascularization model is accelerated by angiogenic oligosaccharides of hyaluronan. Lab Invest. 1995;73: 259–66.
19. Montesano R, Kumar S, Orci L, Pepper MS. Synergistic effect of hyaluronan oligosaccharides and vascular endothelial growth factor on angiogenesis in vitro. Lab Invest. 1996;75:249–62.
20. Obika M, Vernon RB, Gooden MD, Braun KR, Chan CK, Wight TN. ADAMTS-4 and biglycan are expressed at high levels and co-localize to podosomes during endothelial cell tubulogenesis in vitro. J Histochem Cytochem. 2014;62:42–49.
21. Vernon RB, Sage EH. A novel, quantitative model for study of endothelial cell migration and sprout formation within three-dimensional collagen matrices. Microvasc Res. 1999;57:118–33.
22. Taylor CJ, Motamed K, Lilly B. Protein kinase C and downstream signaling pathways in a three-dimensional model of phorbol ester-induced angiogenesis. Angiogenesis. 2006;9:39–51.
23. Suzuki T, Fujikura K, Higashiyama T, Takata K. DNA staining for fluorescence and laser confocal microscopy. J Histochem Cytochem. 1997;45:49–53.
24. Shih SC, Smith LE. Quantitative multi-gene transcriptional profiling using real-time PCR with a master template. Exp Mol Pathol. 2005;79:14–22.
25. Agren UM, Tammi R, Tammi M. A dot-blot assay of metabolically radiolabeled hyaluronan. Anal Biochem. 1994;217:311–5.
26. Davis GE, Camarillo CW. An alpha 2 beta 1 integrin-dependent pinocytic mechanism involving intracellular vacuole formation and coalescence regulates capillary lumen and tube formation in three-dimensional collagen matrix. Exp Cell Res. 1996;224:39–51.
27. Maroski J, Vorderwulbecke BJ, Fiedorowicz K, Da Silva-Azevedo L, Siegel G, Marki A, Pries AR, Zakrzewicz A. Shear stress increases endothelial hyaluronan synthase 2 and hyaluronan synthesis especially in regard to an atheroprotective flow profile. Exp Physiol. 2011;96: 977–86.
28. Jokela TA, Jauhiainen M, Auriola S, Kauhanen M, Tiihonen R, Tammi MI, Tammi RH. Mannose inhibits hyaluronan synthesis by down-regulation of the cellular pool of UDP-N-acetylhexosamines. J Biol Chem. 2008;283:7666–73.
29. Kakizaki I, Kojima K, Takagaki K, Endo M, Kannagi R, Ito M, Maruo Y, Sato H, Yasuda T, Mita S, Kimata K, Itano N. A novel mechanism for the inhibition of hyaluronan biosynthesis by 4-methylumbelliferone. J Biol Chem. 2004;279:33281–9.
30. Kudo D, Kon A, Yoshihara S, Kakizaki I, Sasaki M, Endo M, Takagaki K. Effect of a hyaluronan synthase suppressor, 4-methylumbelliferone, on B16F-10 melanoma cell adhesion and locomotion. Biochem Biophys Res Commun. 2004;321:783–7.
31. Rilla K, Pasonen-Seppanen S, Rieppo J, Tammi M, Tammi R. The hyaluronan synthesis inhibitor 4-methylumbelliferone prevents keratinocyte activation and epidermal hyperproliferation induced by epidermal growth factor. J Invest Dermatol. 2004;123:708–14.
32. Kultti A, Pasonen-Seppanen S, Jauhiainen M, Rilla KJ, Karna R, Pyoria E, Tammi RH, Tammi MI. 4-Methylumbelliferone inhibits hyaluronan synthesis by depletion of cellular UDP-glucuronic acid and downregulation of hyaluronan synthase 2 and 3. Exp Cell Res. 2009;315:1914–23.
33. Edward M, Quinn JA, Pasonen-Seppanen SM, McCann BA, Tammi RH. 4-Methylumbelliferone inhibits tumour

cell growth and the activation of stromal hyaluronan synthesis by melanoma cell-derived factors. Br J Dermatol. 2010;162:1224–32.
34. Jokela TA, Kuokkanen J, Karna R, Pasonen-Seppanen S, Rilla K, Kossi J, Laato M, Tammi RH, Tammi MI. Mannose reduces hyaluronan and leukocytes in wound granulation tissue and inhibits migration and hyaluronan-dependent monocyte binding. Wound Repair Regen. 2013;21:247–55.
35. Montesano R, Orci L. Tumor-promoting phorbol esters induce angiogenesis in vitro. Cell. 1985;42:469–77.
36. Sacharidou A, Stratman AN, Davis GE. Molecular mechanisms controlling vascular lumen formation in three-dimensional extracellular matrices. Cells Tissues Organs. 2012;195:122–43.
37. Ausprunk DH, Boudreau CL, Nelson DA. Proteoglycans in the microvascular. II. Histochemical localization in proliferating capillaries of the rabbit cornea. Am J Pathol. 1981;103:367–75.
38. Queisser KA, Mellema RA, Petrey AC. Hyaluronan and its receptors as regulatory molecules of the endothelial interface. J Histochem Cytochem. 2021;69:25–34.
39. Reeves SR, Kang I, Chan CK, Barrow KA, Kolstad TK, White MP, Ziegler SF, Wight TN, Debley JS. Asthmatic bronchial epithelial cells promote the establishment of a Hyaluronan-enriched, leukocyte-adhesive extracellular matrix by lung fibroblasts. Respir Res. 2018; 19:146.
40. Iruela-Arispe ML, Davis GE. Cellular and molecular mechanisms of vascular lumen formation. Dev Cell. 2009;16:222–31.
41. Neufeld S, Planas-Paz L, Lammert E. Blood and lymphatic vascular tube formation in mouse. Semin Cell Dev Biol. 2014;31:115–23.
42. Charpentier MS, Conlon FL. Cellular and molecular mechanisms underlying blood vessel lumen formation. Bioessays. 2014;36:251–59.
43. Yu JA, Castranova D, Pham VN, Weinstein BM. Single-cell analysis of endothelial morphogenesis in vivo. Development. 2015;142:2951–61.
44. Slevin M, Krupinski J, Gaffney J, Matou S, West D, Delisser H, Savani RC, Kumar S. Hyaluronan-mediated angiogenesis in vascular disease: uncovering RHAMM and CD44 receptor signaling pathways. Matrix Biol. 2007;26:58–68.
45. Shin MR, Kang SK, Kim YS, Lee SY, Hong SC, Kim EC. TNF-alpha and LPS activate angiogenesis via VEGF and SIRT1 signalling in human dental pulp cells. Int Endod J. 2015;48:705–16.
46. Li Y, Zhu H, Wei X, Li H, Yu Z, Zhang H, Liu W. LPS induces HUVEC angiogenesis in vitro through miR-146a-mediated TGF-beta1 inhibition. Am J Transl Res. 2017;9:591–600.
47. Ma B, Dohle E, Li M, Kirkpatrick CJ. TLR4 stimulation by LPS enhances angiogenesis in a co-culture system consisting of primary human osteoblasts and outgrowth endothelial cells. J Tissue Eng Regen Med. 2017;11:1779–91.
48. Bernardini C, Bertocchi M, Zannoni A, Salaroli R, Tubon I, Dothel G, Fernandez M, Bacci ML, Calza L, Forni M. Constitutive and LPS-stimulated secretome of porcine Vascular Wall-Mesenchymal Stem Cells exerts effects on in vitro endothelial angiogenesis. BMC Vet Res. 2019;15:123.
49. Comper WD, Laurent TC. Physiological function of connective tissue polysaccharides. Physiol Rev. 1978; 58:255–315.
50. Laurent TC, Laurent UB, Fraser JR. The structure and function of hyaluronan: an overview. Immunol Cell Biol. 1996;74:A1–7.
51. Balazs EA, Laurent TC. Viscosity function of hyaluronic acid as a polyelectrolyte. J Polymer Sci. 1951;6:665–7.
52. Preston BN, Davies M, Ogston AG. The composition and physicochemical properties of hyaluronic acids prepared from ox synovial fluid and from a case of mesothelioma. Biochem J. 1965;96:449–74.
53. Cleland RL, Wang JL. Ionic polysaccharides. 3. Dilute solution properties of hyaluronic acid fractions. Biopolymers. 1970;9:799–810.
54. Katchalsky A. Polyelectrolyte gels. In: Butler JAV, Randall JT, editors. Progress in biophysics and biophysical chemistry, vol. 4. London: Pergamon;1954. p. 1–59.
55. Strilic B, Eglinger J, Krieg M, Zeeb M, Axnick J, Babal P, Muller DJ, Lammert E. Electrostatic cell-surface repulsion initiates lumen formation in developing blood vessels. Curr Biol. 2010;20:2003–9.
56. Lokeshwar VB, Lopez LE, Munoz D, Chi A, Shirodkar SP, Lokeshwar SD, Escudero DO, Dhir N, Altman N. Antitumor activity of hyaluronic acid synthesis inhibitor 4-methylumbelliferone in prostate cancer cells. Cancer Res. 2010;70:2613–23.
57. Olivares CN, Alaniz LD, Menger MD, Baranao RI, Laschke MW, Meresman GF. Inhibition of hyaluronic acid synthesis suppresses angiogenesis in developing endometriotic lesions. PLoS ONE. 2016;11:e0152302.
58. Twarock S, Reichert C, Peters U, Gorski DJ, Rock K, Fischer JW. Hyperglycaemia and aberrated insulin signalling stimulate tumour progression via induction of the extracellular matrix component hyaluronan. Int J Cancer. 2017;141:791–804.
59. Sironen RK, Tammi M, Tammi R, Auvinen PK, Anttila M, Kosma VM. Hyaluronan in human malignancies. Exp Cell Res. 2011;317:383–91.
60. Chanmee T, Ontong P, Itano N. Hyaluronan: a modulator of the tumor microenvironment. Cancer Lett. 2016; 375:20–30.